The detection of bacterial luciferase in the luminous squid, *Heteroteuthis hawaiiensis*, represents a controversial case in that another species in this genus (*H. dispar*) has been reported to lack symbiotic bacteria (*14*). Ultrastructural examination of the light organs of *H. hawaiiensis* has revealed bacterialike bodies 2 to 3 μm in diameter, yet typical bacteroids were not seen (*15*). On the basis of both ultrastructural data and the inability to cultivate bacteria from the light organ, Dilly and Herring (*14*) suggested that bacteria were not present in the related *H. dispar*; however, they did report the presence of large "bacterialike particles."

The bacterial origin of luminescence in pyrosomes has long been debated (*3*). However, on the basis of ultrastructural analyses of the light organs, it was proposed (*16*) that pyrosomes contain symbiotic luminous bacteria. Our results support the idea that the light is of bacterial origin. The presence of intracellular symbionts, as proposed (*16*), would represent yet another level of integration that the bacterial symbionts have undergone (*17*).

The luminous bacteria–marine animal symbioses represent a continuum of associations, ranging from easily cultured, facultative, extracellular symbionts, to extracellular bacteroid symbionts, to intracellular bacteroid symbionts. This continuum may reflect a gradual integration of the several hosts with the luminous bacteria and could provide a series of model systems for the study of the evolution of symbiosis. The bacterial luciferase assay is a valuable probe in these studies.

GARY LEISMAN
DANIEL H. COHN
KENNETH H. NEALSON
Marine Biology Research Division, Scripps Institution of Oceanography, La Jolla, California 92093

References and Notes

1. W. M. Beebe, *Zoologica (Stuttgart)* **22**, 197 (1937).
2. P. J. Herring and J. G. Morin, in *Bioluminescence in Action*, P. J. Herring, Ed. (Academic Press, New York, 1978), p. 273.
3. E. N. Harvey, *Bioluminescence* (Academic Press, New York, 1952).
4. K. H. Nealson, *Trends Biochem. Sci.* **4**, 105 (1979); _____ and J. W. Hastings, *Microbiol. Rev.* **43**, 496 (1979).
5. J. M. Bassot, in *Bioluminescence in Progress*, F. H. Johnson and Y. Haneda, Eds. (Princeton Univ. Press, Princeton, 1966), p. 557.
6. M. Kessel, *Cytobiologia* **15**, 145 (1977).
7. W. T. O'Day, *Contributions to Science from the Los Angeles County Museum No. 255* (1974).
8. Y. Haneda and F. I. Tsuji, *Science* **173**, 143 (1971).
9. The substrates of the reaction are reduced flavin mononucleotide ($FMNH_2$), oxygen, and one of several long-chain aliphatic aldehydes (RCHO). Oxygen oxidizes the other two substrates in a reaction that yields visible light with a maximum at ~ 490 nm. There is a long-lived enzyme-substrate intermediate that has a half-time of decay on the order of seconds, and any excess $FMNH_2$ autooxidizes to FMN in milliseconds. Thus each enzyme molecule turns over only once during the assay, producing a characteristic kinetic profile (Fig. 1, inset) [K. H. Nealson, *Methods Enzymol.* **57**, 153 (1978)].
10. Luciferase decay kinetics have been examined in extracts of several thousand luminous bacterial isolates independently identified by numerical taxonomy. With no exceptions, members of the genus *Photobacterium* had fast decay kinetics and luminous *Beneckea* isolates had slow decay kinetics [E. G. Ruby, thesis, University of California, San Diego (1977)].
11. In some cases, extensive attempts were made to culture the bacteria using as many as 150 different media. No luminous colonies were ever obtained. In every case some dark colonies did grow on the plates; these were tested for bacterial luciferase activity and all were negative.
12. W. H. Hulet and G. Musil, *Copeia* **3**, 506 (1968); K. Hansen and P. J. Herring, *J. Zool. Proc. Zool. Soc. London* **182**, 103 (1977).
13. Unpublished data cited in (*2*), p. 324.
14. P. N. Dilly and P. J. Herring, *J. Zool. Proc. Zool. Soc. London* **186**, 47 (1978).
15. R. E. Young, personal communication.
16. G. O. Mackie and Q. Bone, *Proc. R. Soc. London Ser. B* **202**, 483 (1978).
17. Pyrosomes flash in response to a variety of stimuli [see (*3*, *7*)]. Since luminous bacteria in culture emit light continuously and those in the transparent pyrosome emit light only upon stimulation, the control of the bacterial light-emitting system may reside in the pyrosome host; the mechanism by which this might occur is unclear.
18. K. H. Nealson, unpublished data.
19. We thank R. E. Young and J. J. Childress for the opportunity to participate in cruises aboard the R.V. *Kana Keoki* (FIDO XII and XIV) and the R.V. *Velero IV*. We thank the crew of the *Cayman Diver* for assistance in collecting specimens. J. McCosker (Steinhart Aquarium) supplied some specimens. T. W. Pietsch identified the ceratioids. M. Haygood, R. Rosson, and B. Tebo helped with specimen collection and enzyme assays. R. E. Young, J. G. Morin, and L. Margulis provided helpful comments on the manuscript. Supported by NSF grant PCM 74-14788.

29 October 1979; revised 9 January 1980

Purinergic Receptors: Photoaffinity Analog of Adenosine Triphosphate Is a Specific Adenosine Triphosphate Antagonist

Abstract. *Arylazido aminopropionyl adenosine triphosphate ($ANAPP_3$), a photoaffinity label, antagonized specifically adenine nucleotide–induced contractions of the guinea pig vas deferens. Irradiation of tissues with visible light in the presence of $ANAPP_3$ resulted in an irreversible antagonism, which was prevented when adenosine triphosphate was present. In the absence of light, the antagonism was reversible and may have resulted from an autoinhibition phenomenon. Responses to acetylcholine, histamine, norepinephrine, and potassium chloride were not affected by $ANAPP_3$.*

There is considerable evidence that many visceral organs of vertebrates are innervated by motor neurons, termed purinergic nerves by Burnstock (*1*), that use adenosine triphosphate (ATP) as a neurotransmitter. Many criteria to establish ATP as a transmitter have been met (*2*). However, a specific pharmacological antagonist to ATP-induced responses (*3*), which would unequivocally demonstrate the existence of purinergic receptors (*4*), has not been available to satisfy the criterion that neurally released ATP is functionally important as a transmitter. One compound, 2,2′-pyridylisatogen, showed promise initially as a selective ATP antagonist (*5*). However, more recent evidence (*6*) indicates that pyridylisatogen has undesirable nonspecific effects.

Arylazido aminopropionyl ATP (3′-*O*-{3-[*N*-(4-azido-2-nitrophenyl)amino]propionyl}adenosine 5′-triphosphate), or $ANAPP_3$, was shown to be a photoaffinity label of rabbit skeletal muscle myosin and F_1-mitochondrial adenosinetriphosphatases (*7*). Being a derivative of ATP, $ANAPP_3$ is, without light activation, a substrate for these enzymes (*7*). Photoactivation with visible light induces a specific covalent attachment to the adenosinetriphosphatase with a resultant decrease in enzyme activity. We reasoned that the photoaffinity characteristics of $ANAPP_3$ might be applied to intact tissues to study the interactions of adenine nucleotides with smooth muscle.

Vasa deferentia from adult guinea pigs were placed in separate water-jacketed glass organ chambers (*8*). $ANAPP_3$ was synthesized by the method of Jeng and co-workers (*7*). The effects of $ANAPP_3$ on concentration-response relationships were evaluated in "light" and "dark" experiments by the following protocols. In light experiments, one tissue of a pair was exposed, in the absence of light, to $ANAPP_3$ for 3 minutes. The $ANAPP_3$ caused an immediate, ATP-like contraction (*9*), which quickly subsided. The tissue was then irradiated in the organ bath for 30 minutes with a tungsten-halogen projector lamp (model DVY, 650 W, 3400 K) (*7*), the filament of which was approximately 10 cm from the tissue. In the presence, but not in the absence, of $ANAPP_3$, irradiation induced a small sustained contraction, at times with cyclic spontaneous contractions superimposed. At the end of photoactivation, fresh bathing medium lacking $ANAPP_3$ was introduced. The remainder of the experiment was begun 4 minutes later and conducted in the dark. In dark experiments, one tissue of a pair was incubated in $ANAPP_3$ for 33 minutes in the

0036-8075/80/0613-1273$00.50/0

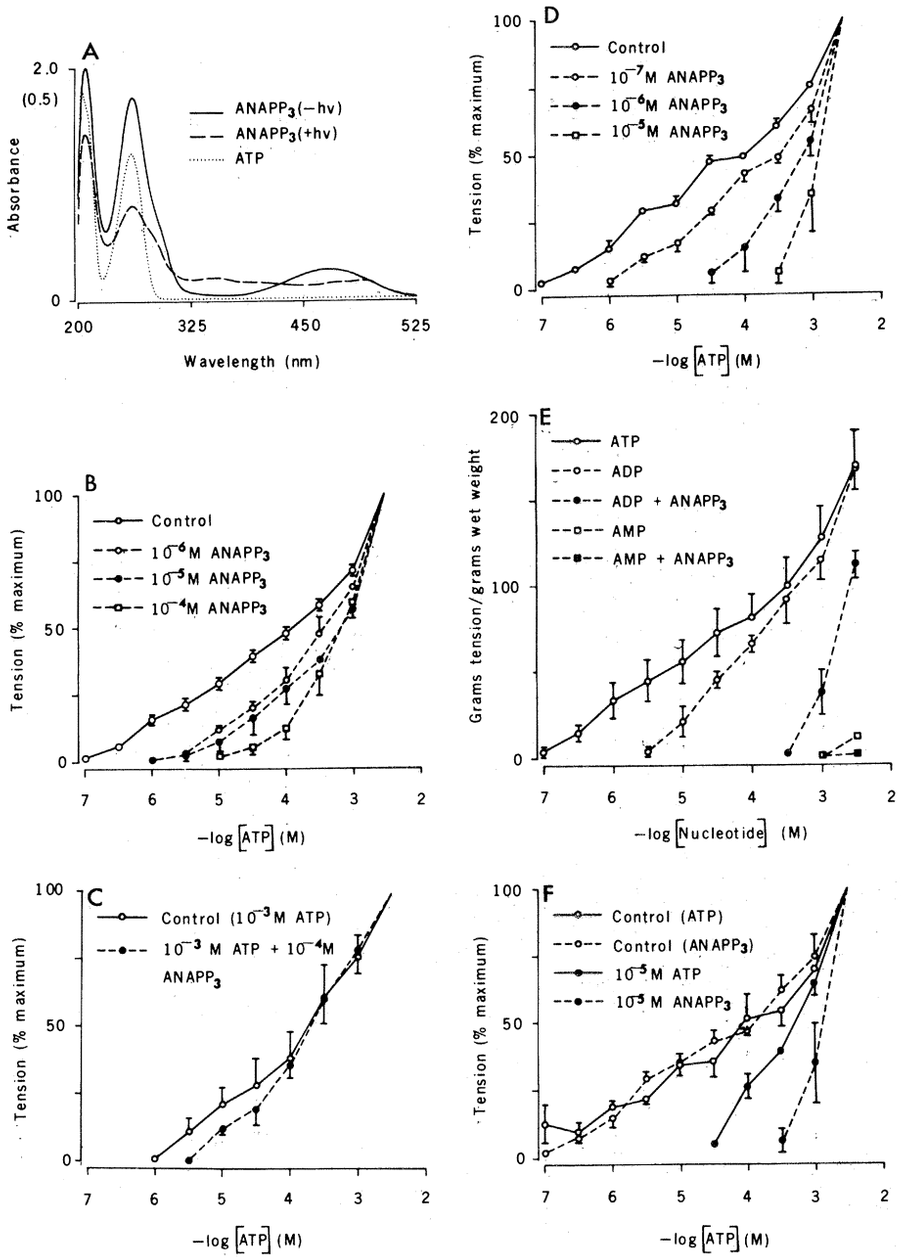

Fig. 1. (A) Spectra of $10^{-4}M$ $ANAPP_3$ in modified Krebs-Henseleit solution collected from organ baths containing vasa deferentia before ($-hv$) and after ($+hv$) photoactivation with the DVY lamp (2.0 full-scale absorbance), and of $2 \times 10^{-5}M$ ATP (0.5 full-scale absorbance). The reference cuvette contained modified Krebs-Henseleit solution. (B) Effect of photoactivated $ANAPP_3$ on the ATP concentration-response relationship (light experiments). The control curve shows control data pooled from individual experiments ($N = 15$). For each concentration of $ANAPP_3$, $N = 5$. No $ANAPP_3$ was present in the bath during the ATP concentration-response determinations. (C) Effect of $ANAPP_3$ ($10^{-4}M$) on the ATP concentration-response relationship after photoactivation in the presence of $10^{-3}M$ ATP. Control: ATP present for 36 minutes and washed out before ATP concentration-response determination ($N = 4$). In treated tissues, ATP was added 3 minutes before $ANAPP_3$ and remained in the bath during irradiation ($N = 4$). Both agents were washed out before the ATP concentration-response determination. (D) Effect of nonirradiated $ANAPP_3$ on the ATP concentration-response relationship (dark experiments). After an incubation period as in light experiments, $ANAPP_3$ remained present in the bath during the entire concentration-response determinations. The control curve shows data pooled from the individual experiments shown ($N = 15$) and from studies using $10^{-8}M$ $ANAPP_3$, which had no effect (results not shown). For each concentration of $ANAPP_3$ illustrated, $N = 4$. (E) Effect of $3 \times 10^{-6}M$ $ANAPP_3$ (nonirradiated) on ADP ($N = 4$) and AMP ($N = 4$) concentration-response relationships. $ANAPP_3$ remained in the bath when the nucleotides were added (dark experiments). For reference, an ATP concentration-response curve is also shown. (F) Comparison of the effects of $10^{-5}M$ ATP ($N = 4$) and $10^{-5}M$ $ANAPP_3$ (nonirradiated; $N = 4$) on the ATP concentration-response curve. Both ATP and $ANAPP_3$ were present during the ATP concentration-response determinations (dark experiments). Controls (no nucleotide present) for both ATP and $ANAPP_3$ are shown.

absence of light. The $ANAPP_3$ was also present for the duration of the concentration-response determinations. For both light and dark experiments, agonists were added 37 minutes after the initial addition of $ANAPP_3$.

Spectrophotometric scans were performed on samples of bathing media collected 33 minutes after the exposure of tissues to $ANAPP_3$ in the absence or presence of light (Fig. 1A). Irradiation induced a change in the absorption spectrum of $ANAPP_3$ (*10*), which is indicative of a presently unknown alteration in $ANAPP_3$ that was produced in the organ bath. The spectra of irradiated and nonirradiated $ANAPP_3$ were qualitatively distinct from that of ATP (see Fig. 1A).

Adenine nucleotides caused contraction of the guinea pig vas deferens (Fig. 1, B to F) (*9*). The observed relative potency was ATP > adenosine diphosphate (ADP) >> adenosine monophosphate (AMP). This order of potency has been observed in other tissues (*4*) in which adenine nucleotides are excitatory agents. Adenosine does not induce contraction in this tissue (*9*) and was not included in the present studies.

Irradiation alone with the DVY visible light source had no effect on the responses of vasa deferentia to mean effective concentrations (EC_{50}) of norepinephrine ($3 \times 10^{-5}M$; $N = 3$), KCl (30 mM; $N = 3$), and ATP ($10^{-5}M$; $N = 3$) (*11*). Responses to norepinephrine ($3 \times 10^{-5}M$; $N = 3$) and KCl (30 mM; $N = 3$) were not affected by $ANAPP_3$ after irradiation. However, following irradiation, $ANAPP_3$ produced concentration-dependent nonparallel shifts of ATP concentration-response curves to the right of the control curve (Fig. 1B). The $ANAPP_3$ did not markedly affect the response to the highest concentration of ATP used. It should be noted that $ANAPP_3$ was not present in the bathing medium during the ATP concentration-response determinations. This suggests that $ANAPP_3$ became irreversibly, perhaps covalently (*7*), bound to the tissue during photoactivation. In separate experiments, responses to repetitive administration of $3 \times 10^{-5}M$ ATP did not return to control levels (up to 2 hours) after the photoactivation and subsequent washout of $10^{-4}M$ $ANAPP_3$ (results not shown).

To determine whether the irreversible antagonism occurred at a nucleotide-specific site, photoactivation was conducted as above but with $10^{-3}M$ ATP added to the organ bath 3 minutes before addition of $10^{-4}M$ $ANAPP_3$. The control organ was exposed to $10^{-3}M$ ATP. After irra-

diation, nucleotide-free bathing medium was introduced, and the remainder of the experiment was performed as described above. The rationale for this experiment was that ATP should compete with $ANAPP_3$ for binding sites in the tissue and protect them from occupation by $ANAPP_3$. Under these conditions, the antagonism by $ANAPP_3$ was prevented (Fig. 1C). This finding is strong evidence for a covalent attachment of $ANAPP_3$ at an ATP-specific agonist site.

Tachyphylaxis to ATP, or autoinhibition (*12*), occurs in many tissues during incubation in the presence of ATP; the phenomenon is readily reversed when ATP is removed. Autoinhibition has been utilized by some workers (*6*, *12*) to determine whether responses to nerve stimulation are reduced to the same degree as those elicited with exogenously added ATP. An important consideration is that antagonism by $ANAPP_3$ after photoactivation differs from ATP autoinhibition in two ways: (i) the antagonism persists when $ANAPP_3$ is no longer present and (ii) repeated washout does not reverse the inhibition.

Since $ANAPP_3$ is a substrate for adenosinetriphosphatase in the absence of light (*7*), we examined the effects of $ANAPP_3$ on concentration-response relationships under these conditions. Surprisingly, $ANAPP_3$ produced concentration-dependent nonparallel shifts of the ATP concentration-response curve to the right of the control curve (Fig. 1D). In fact, $ANAPP_3$ was more potent as an antagonist in the dark than after photoactivation (compare to Fig. 1B) (*13*). It was also a potent antagonist of ADP and AMP in the dark (Fig. 1E). In separate experiments, the antagonism of contractions to $3 \times 10^{-5}M$ ATP by $10^{-5}M$ $ANAPP_3$ was completely reversed 4 minutes after the tissues were washed with $ANAPP_3$-free Krebs solution and remained so for at least 2 hours (results not shown).

Because $ANAPP_3$ was continually present during the concentration-response experiments and the antagonism was reversed by washing, it seemed possible that $ANAPP_3$, like ATP, produced autoinhibition at a nucleotide receptor. Consequently, the effects of $10^{-5}M$ ATP and $10^{-5}M$ $ANAPP_3$ on ATP concentration-response relationships were compared using the dark experiment protocol. Figure 1F shows that the presence of ATP resulted in apparent autoinhibition: the ATP concentration-response curve was shifted to the right of the control curve. By comparison, $ANAPP_3$ produced a nearly tenfold greater shift at the EC_{20} level. The explanation for the greater shift is unknown. The possibility exists that $ANAPP_3$ is more potent than ATP as an autoinhibitory antagonist. Alternatively, the larger rightward shift might be due to the relative potency or efficacy of $ANAPP_3$ compared to ATP as a contraction-producing agonist. This view could not be tested because of the large amount of $ANAPP_3$ required for this type of experiment.

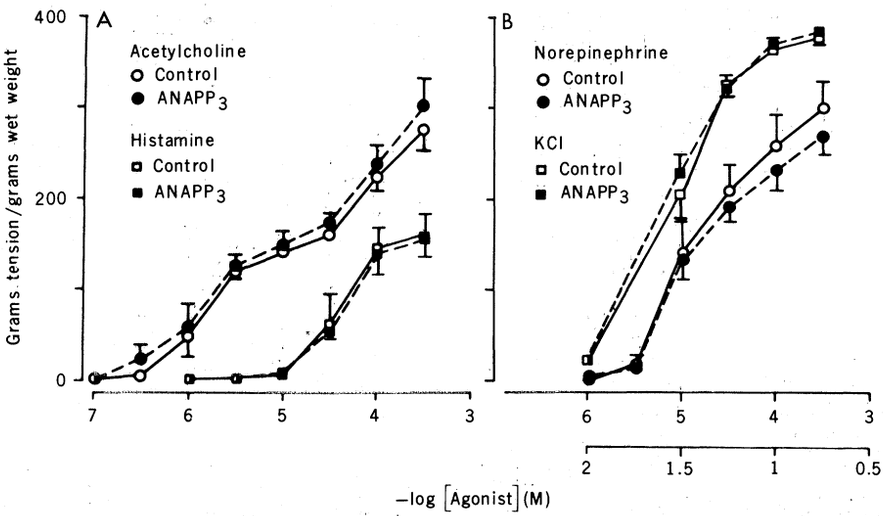

Fig. 2. Effect of nonirradiated $ANAPP_3$ ($3 \times 10^{-6}M$) on concentration-response relationships for (A) acetylcholine and histamine and (B) norepinephrine and KCl (dark experiments). The lower abscissa in (B) gives KCl concentrations. The EC_{50} values for these agents were not affected by $ANAPP_3$ ($P > .05$, Student's t-test; $N = 4$ for each agent). Results shown are means ± standard errors.

Due to the greater apparent antagonistic potency of $ANAPP_3$ compared to ATP, we examined the specificity of the antagonism against several agonists in the absence of light. At $3 \times 10^{-5}M$, $ANAPP_3$ had no effect on the concentration-response curves for acetylcholine, histamine, norepinephrine, and KCl (Fig. 2). Thus, whether the antagonism results wholly or partly from autoinhibition, $ANAPP_3$ without photoactivation is a specific antagonist of adenine nucleotides in the guinea pig vas deferens. Additional parallel studies are needed to determine whether autoinhibition by ATP is as specific.

The specificity of $ANAPP_3$ as an antagonist of adenine nucleotide-induced responses is evidence for the existence of adenine nucleotide receptors. The receptor apparently mediates responses elicited by ATP as well as those caused by ADP and AMP. Thus, the adenine nucleotides may be considered specific agonists, the potency and efficacy of which are determined in part by the number of 5′-phosphates present (*4*).

These results strongly suggest that photoaffinity labels may be valuable probes in studies of intact tissues. By analogy to biochemical studies (*7*), $ANAPP_3$ was initially an agonist (substrate) in the absence of light and became an irreversible antagonist (covalently bound inhibitor) after photoactivation with visible light. A biochemical correlate for the reversible, possibly autoinhibitory, antagonism by $ANAPP_3$ in the dark that was observed in the present study has not been demonstrated.

A logical extension of these studies would be the development of a nucleotide receptor-binding assay. Such assays require a high binding affinity of the receptor for the ligand and slow dissociation of the bound ligand from the receptor. These conditions are not satisfied by $ANAPP_3$ in the dark. However, the irreversible antagonism by photoactivated $ANAPP_3$, which is prevented by ATP, could form the basis for distinguishing specific from nonspecific binding. Because there are many intracellular adenosinetriphosphatases, photoaffinity labeling of the receptor would require using intact tissues.

G. KURT HOGABOOM
Department of Pharmacology and Toxicology, West Virginia University Medical Center, Morgantown 26506
JOHN P. O'DONNELL
School of Pharmacy, West Virginia University Medical Center
JEFFREY S. FEDAN*
Department of Pharmacology and Toxicology, West Virginia University Medical Center, and Physiology Section, Appalachian Laboratory for Occupational Safety and Health, National Institute of Occupational Safety and Health, Morgantown 26505

References and Notes

1. G. Burnstock, *Nature (London)* **229**, 282 (1971); *Pharmacol. Rev.* **24**, 509 (1972); in *Handbook of Psychopharmacology*, L. L. Iversen, S. D. Iversen, S. H. Snyder, Eds. (Plenum, New York, 1975), vol. 5, p. 131; *Neuroscience* **1**, 239 (1976).
2. J. C. Eccles, *The Physiology of Synapses* (Springer-Verlag, Berlin, 1961). See also the 1972 and 1975 reviews by G. Burnstock (*1*).
3. Many drugs affect the response to purine nucleotides, but also have other pharmacological actions: quinidine, imidazoline compounds, and caffeine. See 1972 and 1975 reviews by G. Burnstock for original references (*1*).
4. G. Burnstock, *J. Theor. Biol.* **62**, 491 (1976).
5. M. Spedding, A. F. Sweetmen, D. F. Turner, *Br. J. Pharmacol.* **53**, 575 (1975).
6. D. F. Weetman and N. Turner, *Arch. Int. Pharmacodyn. Ther.* **228**, 10 (1977); G. Burnstock, T. Cocks, R. Crowe, L. Kasakov, *Br. J. Pharmacol.* **63**, 125 (1978); T. Kazic and D. Milosavljevic, *J. Pharm. Pharmacol.* **29**, 562 (1977).
7. S. J. Jeng and R. J. Guillory, *J. Supramol. Struct.* **3**, 448 (1975); J. Russell, S. J. Jeng, R. J. Guillory, *Biochem. Biophys. Res. Commun.* **4**, 1225 (1976). (All the spectra and melting points of the intermediates and $ANAPP_3$ were analogous to those of Jeng and co-workers.)
8. Tissues were bathed for 1 hour in a modified Krebs-Henseleit solution (37°C), which was gassed with 95 percent O_2 and 5 percent CO_2 under 400 mg resting tension. All agonists were added stepwise in increasing concentration at 6-minute intervals. Agonists were present for 2 minutes, and the tissues were washed twice at 2-minute intervals before the next concentration was added.
9. D. P. Westfall, R. E. Stitzel, J. N. Rowe, *Eur. J. Pharmacol.* **50**, 27 (1978).
10. The spectra are identical to those seen in parallel experiments in which $ANAPP_3$ was dissolved in water and scanned before and after irradiation in quartz cuvettes with a UVS-11 Mineralight (253.4 nm; Ultra-Violet Products, Inc.). Irradiation, and not the tissues, caused the spectral changes. Bath temperature remained at 37°C during photoirradiation.
11. Since irradiation with the DVY visible light source had no effect on the tissues, control for light experiments were subsequently not irradiated. Interestingly, exposure of tissues in quartz cuvettes for 30 minutes with 253.4-nm ultraviolet light depressed the response to all concentrations of ATP, and $ANAPP_3$ after photoactivation had no effect under this condition.
12. H. P. Baer and R. Frew, *Pharmacologist* **2**, 273 (1979).
13. One reason for this discrepancy might be that the amount of activable $ANAPP_3$ available in the bath for binding to the tissue began to decline when irradiation was begun. The kinetics of the photoactivation was not studied. The binding of activated $ANAPP_3$ to the tissue would be expected to increase in a time-dependent fashion, in a manner analogous to the interaction of β-haloalkylamines to the α-adrenergic receptor. More effective blockade by $ANAPP_3$ in light experiments might be achieved in future studies by continuously replenishing with $ANAPP_3$ during irradiation.

14. We thank J. L. Mills, Texas Tech University, for mass spectral analysis of $ANAPP_3$ and G. Fromell for expert technical assistance. This work was supported, in part, by training grant T32-GM17039 from the National Institutes of Health.

* Send correspondence to J.S.F.

9 October 1979; revised 8 January 1980

Evidence for a Vesicular Transport Mechanism in Hepatocytes for Biliary Secretion of Immunoglobulin A

Abstract. *Quantitative electron microscopic autoradiography and diaminobenzidine cytochemistry provide evidence for an uptake and vesicular transport mechanism for iodine-125-labeled immunoglobulin A from plasma to bile by hepatocytes in vivo. The data confirm the existence of a hepatobiliary pathway for secretion of immunoglobulin A into the intestine and are consistent with a vesicular transport mechanism for biliary proteins within liver parenchymal cells.*

Immunoglobulin A (IgA) is found in most mammalian secretions, including gut fluid (*1*, *2*). Intestinal IgA is dimeric and possesses the glycoprotein "receptor" referred to as secretory component (*3*, *4*). It has been proposed that this secretory immunoglobulin complex enters gut secretions by traversing small intestinal epithelial cells from the site of its synthesis by plasma cells in the lamina propria (*5*). Recently, secretory IgA was found in normal rat bile (*6–8*). Fisher *et al.* (*7*) showed that rat liver has an extraordinary capacity to remove polymeric IgA devoid of secretory component from portal blood and to secrete it into bile complexed to secretory component.

To investigate the morphological mechanisms involved in the transport of IgA into bile, dimeric IgA was prepared from rat myelomas (*7*) and labeled with ^{125}I to a specific activity of 0.1 μCi/μg. Purified labeled IgA (35 μCi) was injected either alone or with horseradish peroxidase (HRP) (10 mg per 100 g of body weight) directly into the portal veins of fasted male Sprague-Dawley rats weighing 250 to 300 g. Horseradish peroxidase provides a useful non-receptor-mediated marker for endocytically derived vesicles (*9*, *10*). One and 30 minutes after being injected, the livers were perfusion-fixed with glutaraldehyde and paraformaldehyde and then processed for light and electron microscopic autoradiography and diaminobenzidine cytochemistry to demonstrate HRP (*9*). To assess the secretion of IgA into bile, the common bile duct was cannulated with PE-10 tubing (Clay-Adams) and bile was collected at 10-minute intervals for 2 hours. Radioactivity from the labeled IgA was determined by counting equal portions of bile with a gamma counter. The HRP in the bile was assessed by observing the spectrophotometric change in absorbance due to oxidation of *o*-dianisidine at 460 nm (*11*). The density of silver grains revealed by autoradiography was determined by using two half-distances for all associations (*9*, *12*).

One minute after injection of the proteins, electron microscopic autoradiography showed grains associated primarily with the sinusoidal plasma membranes of parenchymal cells (Fig. 1). Thirty minutes after the injection, grains were observed over hepatic parenchymal cell cytoplasm but were concentrated over bile canalicular regions (Fig. 2). Quantitative electron microscopic autoradiography showed grains associated with sinusoidal hepatocyte plasma membranes and forming endocytic vesicles (58 percent), and with endocytic vesicles approximately 1000 Å in diameter within the cell (7 percent), as determined by their content of HRP 1 minute after the injection (Table 1). Grains were associated, to a lesser extent, with other subcellular organelles in the hepatocytes (Table 1). After 30 minutes, the number of grains near hepatocyte plasma membranes declined to 10 percent, whereas those associated with HRP-containing endocytic vesicles 1000 Å in diameter, now located in the interior of the cell, increased to 26 percent (Table 1). These grains and the associated vesicles were abundant around bile canaliculi, and vesicles were occasionally observed fusing with the bile canalicular membrane. Grains associated with other organelles were also observed (Table 1). In the ab-

Table 1. Association of silver grains with organelles in the hepatocytes. Approximately 300 grains were counted at each time.

Organelle	Distribution of grains (%)		Organelle volume per unit volume of hepatocyte (%)
	1 minute after protein injection	30 minutes after protein injection	
Plasma membrane	58	10	
Endocytic vesicles	7	26	1
Smooth endoplasmic reticulum	14	35	8
Rough endoplasmic reticulum	6	8	6
Mitochondria	5	5	19
Nucleus	3	3	8
Golgi-rich area	1	1	3
Lysosomes	1	3	< 1

0036-8075/80/0613-1276$00.50/0